

# Platelet rich fibrin versus ozone gel for periodontal regeneration in induced rats' intrabony three-wall periodontal defects

Aya Anwar Alsherif\*, Heba Mohamed Eltokhey, Doaa Ameen Taiema

Oral Biology Department, Faculty of Dentistry, Tanta University, Tanta, Egypt

## ARTICLE INFO

**Keywords:**  
 Periodontium  
 Periodontitis  
 Three wall periodontal defect  
 Ozone therapy  
 Platelet rich fibrin

## ABSTRACT

**Background:** The question of whether platelet rich fibrin and ozone can enhance regeneration of periodontal defect was addressed.

**Materials and methods:** three-wall periodontal defects were surgically created in 30 rats involving mesial aspect of right mandibular first molar. Rats were randomly assigned into three groups: 1) Group I (Positive control group). 2) Group II (Ozone treated group) and 3) Group III (PRF treated group). Two weeks after surgery, five rats from each group were euthanized and the remaining was euthanized 4 weeks post surgery. The degree of periodontal regeneration was evaluated using light microscope and scanning electron microscope. Histomorphometric measurements and anti-PCNA immunohistochemical counting were statistically analyzed.

**Results:** group I showed intense inflammatory reaction with mild new bone formation. In group II, partial regeneration was seen with moderate new woven bone formation in 2 weeks period. After 4 weeks, almost complete restoration of periodontium was seen. In group III, after 2 weeks, moderate lamellar bone formation was observed. In 4 weeks period, the periodontal regeneration was almost completed. Histomorphometric analysis showed a significant difference between group I and group II. The difference between group I and group III was significant in 2 weeks and highly significant after 4 weeks. That between group II and group III was nonsignificant in 2 weeks and significant in 4 weeks. Anti-PCNA analysis was nonsignificant between groups.

**Conclusions:** both Platelet rich fibrin and ozone can improve histological parameters associated with healing of experimental intrabony periodontal defects in rats with the former being superior.

## 1. Introduction

The periodontium, from the Greek terms *peri-*, meaning “around” and *-odont*, meaning “tooth”, is a combined term created to designate the totality of tissues which anchor the teeth to the jaw bone. It consists dominantly of four major components; dentogingival junction, periodontal ligament (PDL), cementum and the alveolar bone. They collectively constitute and function as a developmental, biological and functional unit to keep the tooth in its position despite varying responses during mastication.<sup>1–3</sup>

Periodontitis is an inflammatory disease that causes pathological alterations in this tooth-supporting complex.<sup>4,5</sup> It begins with inflammation of the gingiva which represents the body's response to certain bacteria that have been allowed to accumulate on the teeth. Although it is a part of the body's defense system, this inflammatory response can eventually cause serious damage as if the problem is not treated, the inflammation will spread along the roots of the teeth causing destruction of PDL and supporting alveolar bone and finally

potential loss of teeth.<sup>6</sup>

Nonsurgical and conventional surgical periodontal therapies may result in successful clinical outcomes such as probing depth reduction and gain of clinical attachment. However, histologically, the healing following these treatment approaches mostly showed the damaged tissues to be replaced by tissue that doesn't typically duplicate the function of the original one.<sup>7–9</sup>

To date, several regenerative procedures have been developed in an attempt to treat periodontitis.<sup>10–12</sup> However, the current therapeutic techniques used, either alone or in combination, have limitations in producing a true regeneration especially in advanced periodontal defects.<sup>13–15</sup> This had led to the necessity to find a regenerative material that can comprehensively regenerate the periodontium with development of a whole new attachment apparatus.

Ozone therapy can be defined as a versatile bio-oxidative therapy in which ozone is administered as gas or dissolved in water or oil base to obtain therapeutic benefits. It is characterized by minimally invasive and conservative application, low cost, no side effects and restricted

\* Corresponding author.

E-mail addresses: [alsherif\\_aya@yahoo.com](mailto:alsherif_aya@yahoo.com) (A.A. Alsherif), [eltokheyheba@yahoo.com](mailto:eltokheyheba@yahoo.com) (H.M. Eltokhey), [dodofirstmolar@gmail.com](mailto:dodofirstmolar@gmail.com) (D.A. Taiema).

<https://doi.org/10.1016/j.jobcr.2020.09.001>

Received 29 June 2020; Received in revised form 22 August 2020; Accepted 2 September 2020

Available online 04 September 2020

2212-4268/ © 2020 Published by Elsevier B.V. on behalf of Craniofacial Research Foundation.

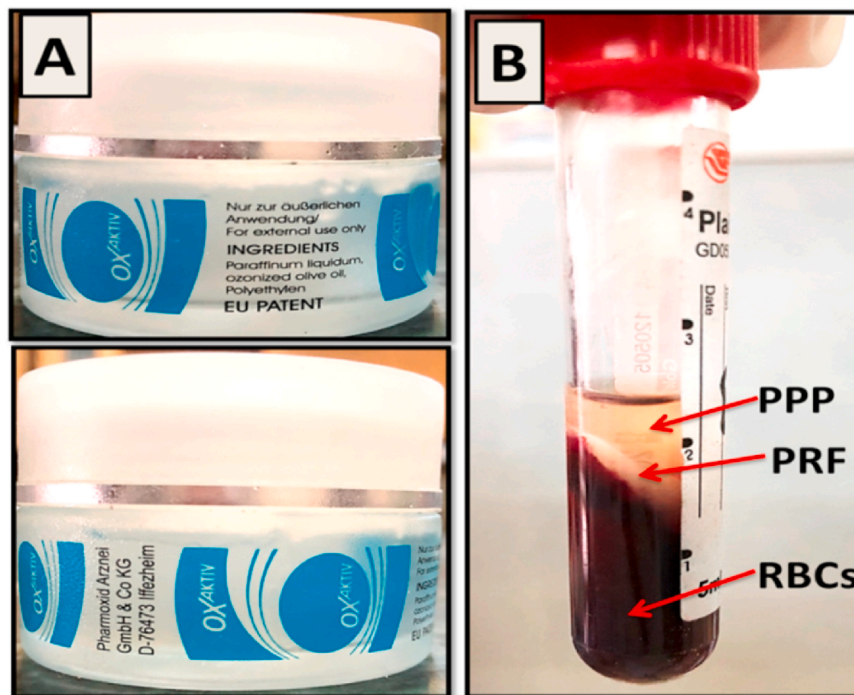


Fig. 1. (A); Ozone gel (OXaktiv) ingredients and manufacturing. (B); PRF preparation with the PRF clot interposed between PPP and RBCs.

intolerance or contraindication.<sup>16</sup>

This therapeutic approach proved to have the ability of treating various diseases owing to ozone's remarkable antimicrobial,<sup>17–19</sup> anti-hypoxic,<sup>20</sup> biosynthetic<sup>21</sup> and immunostimulating<sup>22</sup> properties. Such unique features justify the current interest in ozone application as an alternative treatment for many acute and chronic diseases.<sup>23–25</sup>

In the field of periodontics, the effect of ozonated water on oral microorganisms and dental plaque was studied and amazingly, it was found to have the ability to kill gram-positive, gram-negative oral microorganisms and oral *Candida albicans*.<sup>26</sup> Accordingly, ozone therapy presents great advantages when used as a support for conventional treatments and is strongly recommended for use in a wide range of dental specialties, particularly periodontics.<sup>27</sup>

On the other hand, nowadays, most of researches are being focused on the development of therapeutic periodontal alternatives which are easy to prepare, biocompatible to living tissues, economically cheap and have the ability to release growth factors thus accelerating hard and soft tissue healing.<sup>28</sup>

Many trials are made in the field of regenerating damaged periodontal tissues. These include strategies with graft materials like allografts, xenografts or alloplasts. Although many of these materials have shown promise in different aspects of regenerative medicine, they all, sometimes, create a "foreign body reaction" when introduced into human body.<sup>29</sup>

In addition, while many of these available biomaterials carry properties needed for regeneration, very few of them have the potential to promote angiogenesis directly to the damaged tissues.<sup>29</sup>

An emerging point of view thought that the complex nature of the oral tissues, with neighboring hard and soft tissue components both of which possess unique cells through specialized extracellular matrix,<sup>30,31</sup> is too difficult to be imitated by using usual chemical scaffolds and stem cells. So, up to date methodologies prefer natural scaffolds that are more likely to be repopulated by the patient's own stem cells thus finally generating a perfect autologous tissue-engineered organ.<sup>32</sup> One such complex autologous natural scaffold is PRF.

PRF, as described by Choukroun et al.,<sup>33</sup> is a second-generation platelet concentrate which contains platelets, leukocytes and growth factors in the form of fibrin membrane prepared from the patient's own

blood free of any anticoagulant or other artificial biochemical modifications. The PRF clot forms a strong natural fibrin matrix, which concentrates almost all the platelets and growth factors of the blood harvest.<sup>34,35</sup>

Regarding its medical applications, several studies had shown its synergistic effect in wound healing,<sup>36,37</sup> angiogenesis,<sup>38</sup> neoossification<sup>39–41</sup> and osteoblastic proliferation and differentiation.<sup>42,43</sup>

Recently, many literatures suggest the potential role of PRF in periodontal regeneration and tissue engineering depending on its ability to create an improved space making effect which facilitates cellular events favorable for periodontal regeneration and mineralized tissue formation. Also, the platelet derived growth factor (PDGF) was found to have an important role in periodontal regeneration and wound healing<sup>44</sup> with its receptors being localized on gingiva, periodontal ligament and cementum where it functions as a chemo attractant for fibroblasts and osteoblasts and induces their activation.<sup>45,46</sup>

Based on these assumptions, we investigated the capability of PRF versus ozone gel for periodontal regeneration in a common type of periodontal disease, induced intrabony three-wall periodontal defects, in rats.

## 2. Materials and methods

### 2.1. Experimental animals and sample assignment

A sample of thirty rats was chosen according to certain inclusion criteria with standardization of all confounding variables (healthy, adult, male, Wistar albino rats, weighting about 300–360 g and about 3–4 months old). Our study was designed in accordance with the guidelines for the responsible use of animals in research as a part of scientific research ethics recommendation of Ethical Committee at Faculty of Dentistry, Tanta University, Egypt. The rats were kept in separate cages under the same controlled conditions of temperature and humidity with a 12-h day/night cycle. They were also served a standard laboratory diet twice daily and had free access to tap water.

The Animals were randomly assigned into three groups as follows: 1) *Group I* (Positive control group, n = 10). 2) *Group II* (Ozone treated group, n = 10) and 3) *Group III* (PRF treated group, n = 10).

## 2.2. Experimental materials

1. Ozone gel (OXaktiv, Pharmoxid Arznei, GmbH & Co KG., Germany): its constituents include paraffin liquidum, ozonized olive oil and polyethylene (Fig. 1-A).
2. Autologous PRF membrane (Fig. 1-B).

### 2.2.1. PRF preparation

The classical Choukroun's technique for PRF preparation was strictly followed.<sup>33</sup> A 4-ml blood sample was obtained from the orbital sinus of each rat of the corresponding group using a hematocrit tube. It was collected in a plain tube and immediately centrifuged at 2000 rpm (approximately 400 g) for 10 min. After centrifugation, the resultant product consisted of three layers; the topmost layer of acellular supernatant platelet poor plasma (PPP), PRF clot in the middle and RBCs at the bottom of the test tube (Fig. 1-B). The PRF clot was immediately withdrawn from the tube using sterilized tweezers and the attached RBCs were mechanically separated and discarded using a sterilized scissor. PRF clot was then placed between two layers of sterile gauze with gentle pressure applied to squeeze fluids out thus finally obtaining PRF membrane.<sup>47</sup>

## 2.3. Surgical procedures

Unilateral three wall intrabony defect was created mesial to the right mandibular first molars of all rats as described in details by Yu et al.<sup>48</sup> The surgery was performed under general anesthesia. After food and water deprivation for 12 h, each animal was weighed and anesthetized with an intramuscular injection of ketamine chlorhydrate (Rotexmedica, Trittau, Germany) 0.06 mg/L per kg body weight and 2% xylazine hydrochloride (Xylaject, Adwea, Egyptian international pharmaceutical industries, 10th of Ramadan, city area, Egypt) 0.03 mg/L per kg body weight.

The animals were placed on the left lateral recumbency position and the area of incision was disinfected with Betadine antiseptic solution (Povidone-iodine 10% w/v. El Nile co. for pharmaceuticals and chemical industries, Cairo, A.R.E.). Then, a 3-mm-long full-thickness incision was made on the alveolar ridge mesial to the right mandibular first molar (Fig. 2-A). Minimal buccal and lingual mucoperiosteal flaps were raised to expose the associated alveolar bone (Fig. 2-B) and, under continuous water irrigation, a three wall intra bony defect was surgically created using a low speed hand piece with a 1 mm diameter round diamond bur to remove the mesial wall of alveolar bone socket of the right mandibular first molar (Fig. 2-C). The dimensions of the defect were constantly monitored using a clinical periodontal probe until the required size and contour was obtained ( $W \times L \times D$ ;  $2 \times 2 \times 1$ , 5 mm) (Fig. 2-D). Root planing was carried out on the exposed root surface using hand periodontal curette to remove the residual bony spicules and PDL fibers. The defect area was copiously rinsed with saline to remove any debris then the root surface was thoroughly dried with sterile gauze.

After completion of the surgery, in Group I, the mucoperiosteal flap was repositioned and sutured with resorbable interrupted suture (vicryl 5/0, International Sutures Manufacturing Co. Egypt) to achieve primary closure. The same was achieved in group II & III after treatment application as illustrated in (Fig. 3).

To prevent postoperative infection, ceftriaxone (Xoraxon, Medical Union Pharmaceuticals, Egypt) was given to the animals as intramuscular injections for 3 days. 2 weeks after surgery, five rats from each group were euthanized using overdose of anesthesia. The remaining rats were euthanized 4 weeks post surgery.

## 2.4. Histological processing

After sacrifice, the animals had their mandible excised and the defect area was dissected using low speed hand piece with double sided

diamond disc. Excess tissues were removed then the specimens were fixed in 10% buffered formalin for 48 h followed by decalcification in 10% EDTA. The specimens were then dehydrated, infiltrated with paraffin and finally embedded in paraffin block. Serial mesio distal longitudinal sections (5  $\mu$ m in thickness), from the central portion of the defect, were cut with a microtome (LEICA, RM 2245, Germany) for Haematoxylin–Eosin (H&E) and anti-PCNA immunohistochemical staining.

### 2.4.1. Histomorphometric analysis

Six specimens per each group, three per each time interval, were incorporated in this analysis. Images of four H&E-stained sections from the central portion of the defect area of each specimen were taken at the same magnification (x100) for quantitative evaluation of alveolar bone regeneration. The images were captured using Light Microscope built in camera (LEICA ICC50 HD Camera system) via image software LAS EZ version 3.0.0.

Surface area measurement was performed on the images using the Image J analysis software (Image J 1.42q, Wayne Rasband, USA) as follows<sup>49</sup>:

- New bone area (NBA/ $\mu$ m<sup>2</sup>): represented by the area of newly formed alveolar bone within a standardized area of interest (AoI).

## 2.5. Scanning electron microscopic assessment

The defect areas were dissected from the mandible and the soft tissue covering bone was mechanically removed. Tissue specimens were fixed in 2% glutaraldehyde at pH 7.4, dehydrated then gold plated using JFC-1100E ion Sputtering device to be analyzed using scanning electron microscope (JSM-IT200, JEOL).

## 2.6. Statistical analysis

For statistical analysis of anti-PCNA immunostained slides, six specimens per each group, three per each time interval were involved. Images of four histological sections from each specimen were captured, under magnification x200, and analyzed using Image J Analysis System Software. The number of anti-PCNA-positive nuclei was counted in an area of 1000  $\mu$ m  $\times$  1000  $\mu$ m in the central area of the periodontal defect.<sup>50</sup>

The quantitative data of both histomorphometric and immunohistochemical analyses were collected, tabulated and statistically analyzed using CO-STAT analysis (version 6.4). Numerical variables were expressed by descriptive statistics as mean, standard deviation and range. One way ANOVA and post hoc test (tukey-test) were used to compare quantitative data between groups in both treatment time intervals.

## 3. Results

### 3.1. Histological analysis

In **group I**, in 2 weeks period, H & E stained sections showed persistence of the periodontal defect with enlargement of the defect area in all specimens. This was accompanied with severe destruction of the periodontal apparatus and intense inflammatory cells infiltration (Fig. 4-A). The upper border of the defective alveolar bone showed a small area of newly formed woven bone separated from the preexisting bone by accentuated reversal line. Many osteoclasts were seen in relation to the highly irregular bone surface (Fig. 4-B).

In 4 weeks period, all specimens showed continuation of the periodontal inflammation, however, with a mild decrease in the width of the periodontal defect area. A small isolated newly formed bony island was detected just below the root apex (Fig. 5-A). On a higher magnification, the trabeculae of this bone island appeared to extend almost reaching the root apex with its surface lined by apparent osteoblastic

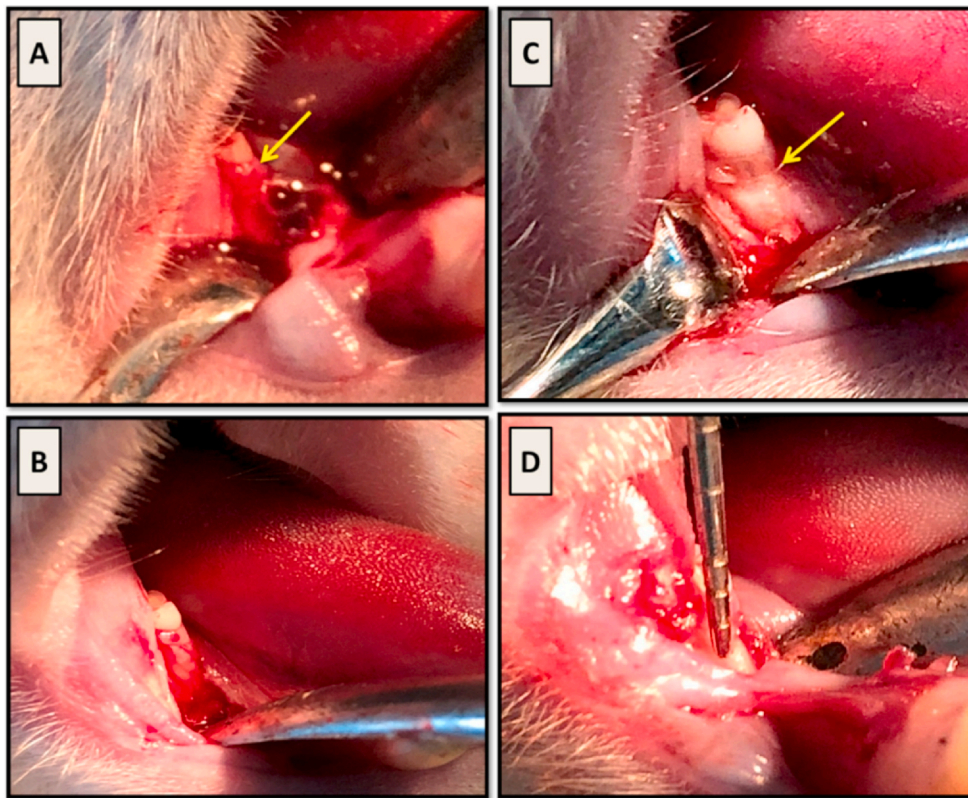


**Fig. 2.** (A); a 3- mm long full thickness incision was made mesial to right mandibular first molar (*arrow*). (B); the mucoperiosteal flap was raised to expose alveolar bone related to mesial root surface (*arrow*). (C); creation of the periodontal defect with exposure of the mesial root surface (*arrow*). (D); a periodontal probe was used to monitor the defect size.

activity (Fig. 5-B). Non functionally oriented collagen fibers were seen in the PDL area and the gingival epithelium had proliferated and migrated deeply into the underlying granulation tissue. Formation of long junctional epithelium was reported in some specimens. Root resorption was seen in all specimens of this group in both 2 and 4 weeks follow up

periods.

In **group II**, in 2 weeks period, partial regeneration of the periodontal apparatus, with partially recovered dentogingival junction (DGJ), was observed in most specimens (Fig. 6-A). Moderate new bone formation of woven pattern was seen on the crest of the alveolar bone

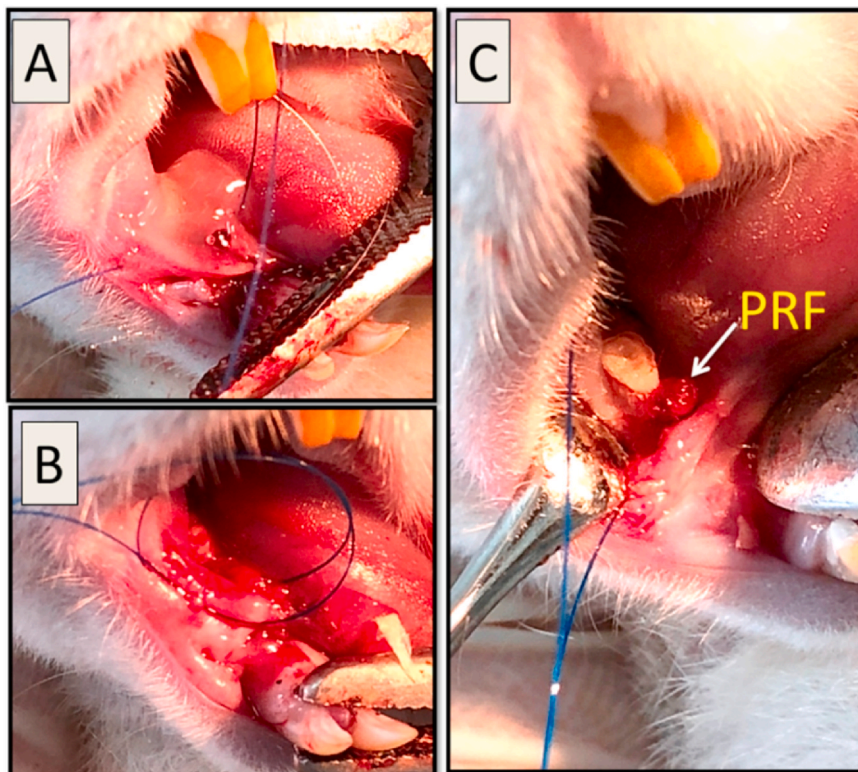


**Fig. 3.** (A); In Group II, a 1 mg of ozone gel was accurately applied over the defect area with a sterile syringe. (B); In Group III, after defect creation, a stitch was first taken in relation to the defect but left un-knotted. (C); the PRF membrane (*arrow*) was positioned over the defect area then the stitch was immediately knotted over it. This step was important to ensure that PRF membrane won't be displaced during suturing.

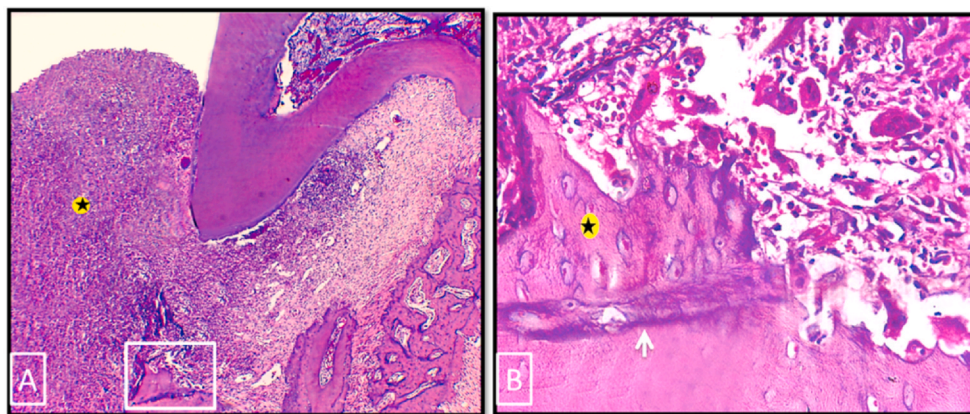


**Fig. 4.** Photo micrographs of group I (2 weeks period). (A) showing enlargement of the defect area with intense inflammatory cell infiltration (*asterisk*). (B) A higher magnification of the boxed area of A showing the upper border of the defective alveolar bone. A small area of newly formed woven bone (*asterisk*), with characteristic large numerous osteocytes, was separated from old bone by accentuated reversal line (*white arrow*). Many osteoclasts were seen occupying their Howship's lacunae on the upper border of alveolar bone. (H&E stain, original magnification A  $\times 100$ , B  $\times 400$ ).

where it was separated from the old bone by accentuated reversal line. Regular osteoid layer was seen outlining the newly formed bone with no signs of osteoclastic activity (Fig. 6-B). Insertion of newly formed PDL Sharpey's fibers into the bone surface was also detected (Fig. 6-C). No resorption cavities were detected on the root surface of any specimen.

After 4 weeks, almost complete restoration of the normal architecture of periodontium was seen with reestablishment of DGJ. The alveolar bone was almost completely renewed with its crest approaching the same level of that of the interradicular septum. The newly regenerated bone appeared to have a mature dense lamellar pattern with accentuated several reversal lines and active plump osteoblasts outlining its surface. Concerning PDL space, it was completely filled with dense fibrous connective tissue. The alveolar crest, horizontal and oblique groups of PDL, together with the dentoperiosteal group of gingival ligament, were regenerated (Fig. 7).

In group III, after 2 weeks, the whole defect area was almost obliterated by newly regenerated periodontal tissues with full reestablishment of DGJ. All specimens of this group showed a significant restoration of the normal architecture of PDL with identification of alveolar crest and horizontal groups of PDL. Numerous active fibroblasts together with wide interstitial tissue spaces were also observed throughout the regenerated periodontal tissue. The regenerated alveolar bone had a mature lamellar structure that was outlined by a uniform osteoid layer and active plump osteoblasts (Fig. 8-A&B). There were no instances of epithelial down growth, ankylosis or root resorption.

In 4 weeks follow up period, the defective bony wall was almost completely regenerated to a level almost reaching that of the interradicular septum. A faint reversal line was seen separating the regenerated bone from the older bone. (Fig. 8-C).

The normal architecture of PDL was ideally restored. The new collagen fiber bundles were grouped into the well-defined functionally oriented principal fibers of PDL with regeneration of alveolar crest, horizontal and oblique groups. The dentogingival junction was completely renewed with easy recognition of dentogingival and dentoperiosteal groups of gingival ligament (Fig. 8-D).

### 3.2. Scanning electron microscopic analysis

In group I, in 2 weeks period, the three-wall intrabony defect was evident with exposure of the mesial aspect of the right mandibular first molar. A higher magnification revealed rough surface with many Howship's lacunae. However, scattered small newly formed bony speckles could also be detected (Fig. 9-A&B).

In 4 weeks, SEM evaluation showed persistence of the intrabony defect, however, a mild new bone formation was seen. On a higher magnification, it showed woven structure consisting of randomly oriented collagen bundles with many prints representing spaces that were previously occupied by osteoblasts. (Fig. 9-C&D).

In group II, after 2 weeks, healing of the bone defect was observed to a level almost covering the apical half of the exposed root surface. A higher magnification showed somewhat smooth outer surface with irregularly outlined neurovascular canals' orifices (Fig. 10).

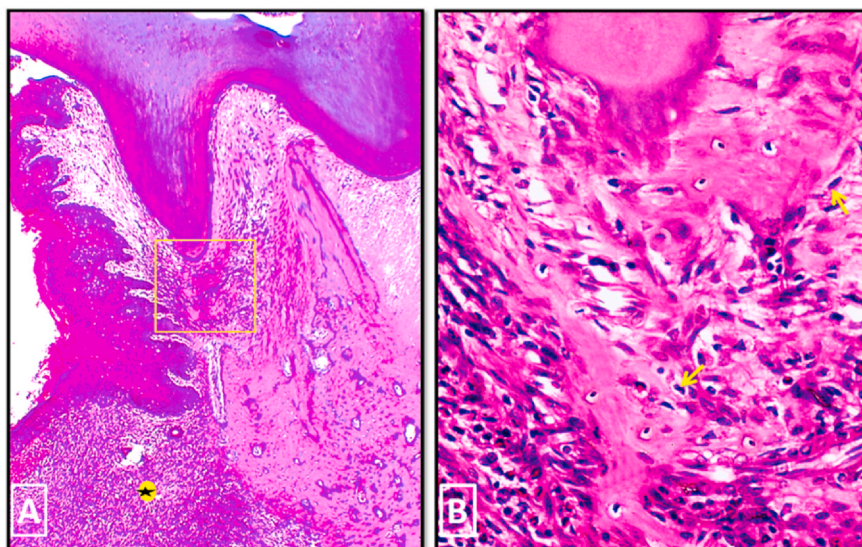


**Fig. 5.** Photo micrographs of group I (4 weeks period). (A) showing narrowing of the defect area with persistence of inflammatory cells infiltration (*asterisk*) and obvious proliferation of the gingival epithelium. (B) A higher magnification of the boxed area of A showing the close approximation of the bony island to the root apex with its surface lined by apparent osteoblastic activity (*yellow arrows*). (H&E stain, original magnification A  $\times 100$ , B  $\times 400$ ).

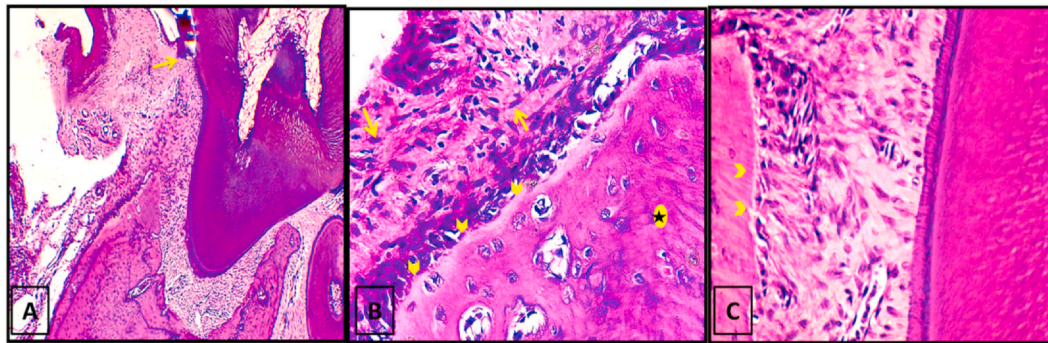


**Fig. 6.** Photo micrographs of group II (2 weeks period). (A); showing partial regeneration of the periodontal apparatus with partial re-establishment of DGJ (yellow arrow). (B); A higher magnification of the outer bone surface of A. The newly formed woven bone (black asterisk) was covered by regular osteoid layer (yellow arrowheads). No signs of osteoclastic activity were seen. Numerous fibroblasts were located in the connective tissue adjacent to the bone surface (yellow arrows). (C); A higher magnification of the inner bone surface and PDL area of A. Note the insertion of newly formed PDL fibers (Sharpey's fibers) in the regenerated bone (yellow arrow heads). (H&E stain, original magnification A x100, B & C x400).

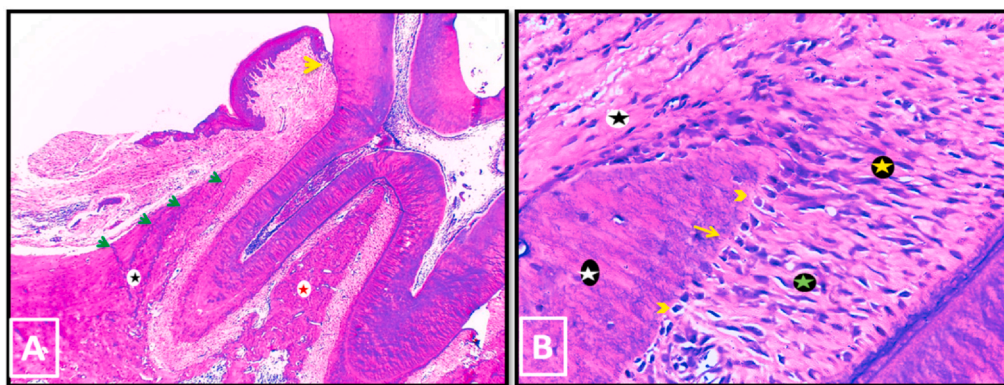


**Fig. 7.** Photo micrographs of group II (4 weeks period). (A); the mesial alveolar bony wall was almost completely regenerated (black asterisk) with its crest approaching the same level of that of the interradicular septum (red asterisk). Several reversal lines were seen (green arrows). DGJ was reestablished (yellow arrow). (B); A higher magnification showing the dense lamellar structure of the new bone (white asterisk). Functionally oriented alveolar crest group (yellow asterisk), horizontal group of PDL (green asterisk) and dentoperiosteal group of gingival ligament (black asterisk) were renewed. Note the inserting Sharpey's fibers (yellow arrow) with plump osteoblasts on the bone surface (yellow arrowheads). (H&E stain, original magnification A x100, Bx400).

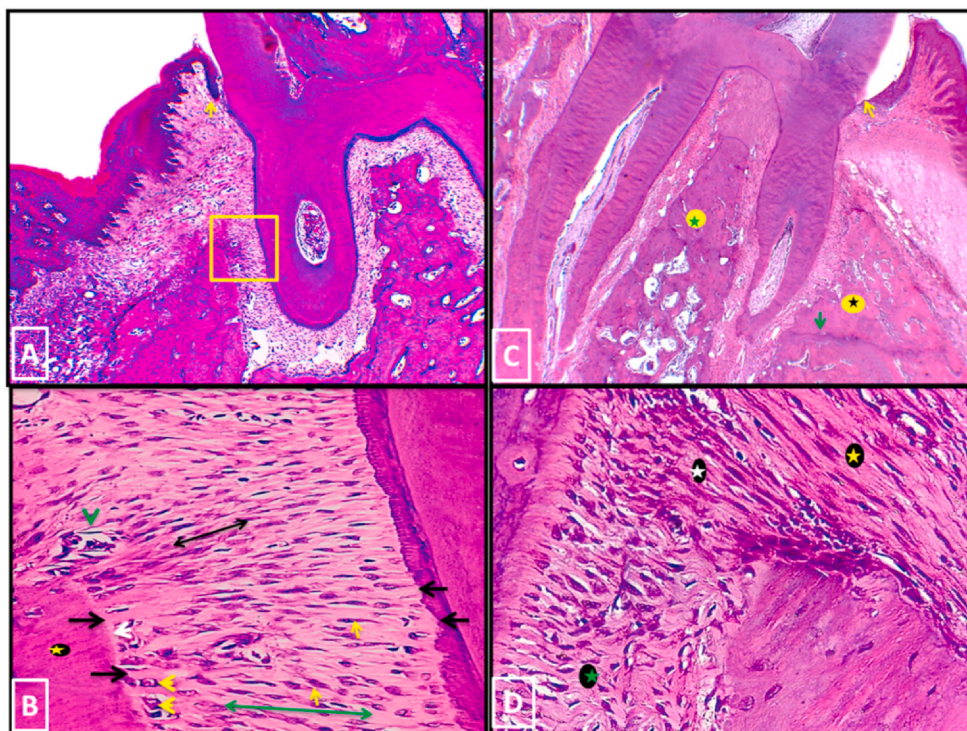


**Fig. 8.** Photo micrographs of group III (A, B: 2 weeks period, C, D: 4 weeks period). (A); the whole defect area was almost obliterated by newly regenerated periodontal tissues. Yellow arrow: reestablished DGJ. (B) a higher magnification of the boxed area of A. The regenerated lamellar alveolar bone (yellow asterisk) was covered with thin uniform osteoid layer (white arrow) and active osteoblasts (yellow arrow heads). Fibroblast like cells (Yellow arrows) spread throughout the PDL area. Alveolar crest group (black double sided arrow) and horizontal group (green double sided arrow) of PDL were detected. Black Arrows: Sharpey's fibers attachment, green arrowhead: blood vessel. (C); The mesial wall of alveolar bone (black asterisk) was regenerated to a level almost reaching that of the interradicular septum (green asterisk). Note reestablished DGJ (yellow arrow). (D); A higher magnification of A showing functionally oriented groups of PDL. white asterisk: alveolar crest group, green asterisk: horizontal group, yellow asterisk: dentoperiosteal group of gingival ligament. (H&E stain, original magnification A & Cx100, B & Dx400).

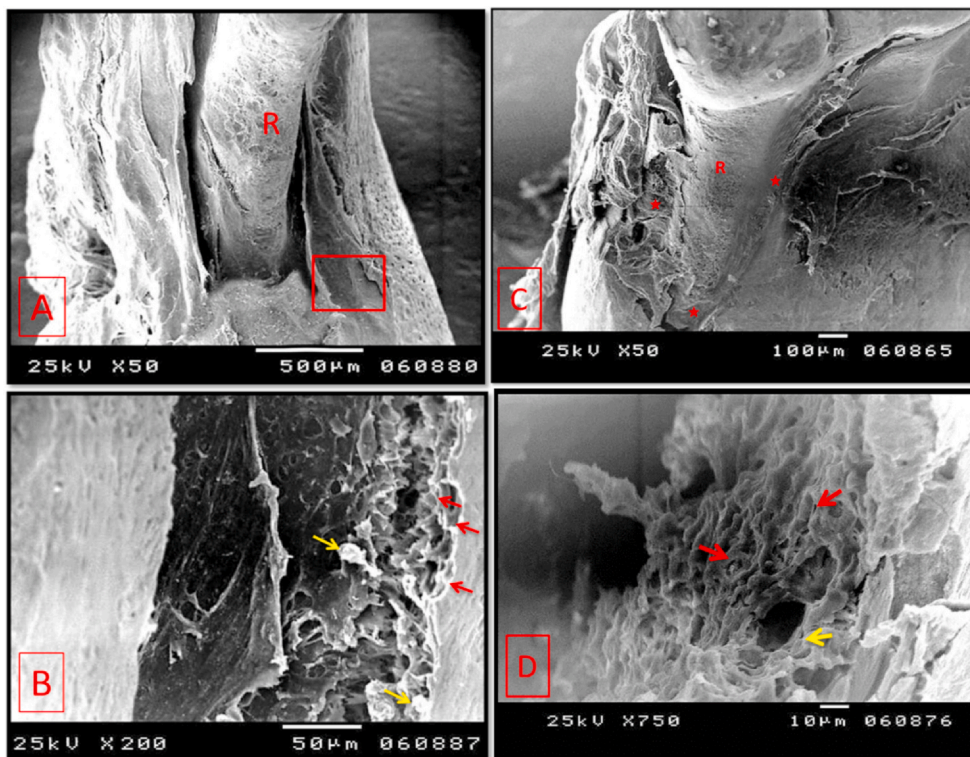


**Fig. 9.** Scanning electron micrographs of group I (A & B: 2 weeks period, C & D: 4 weeks period). (A); showing the three wall intrabony defect. (B); A higher magnification of the boxed area of A showing many Howship's lacunae (red arrows). Few small newly formed bony specules could also be seen (yellow arrows). (C) The majority of the mesial root surface was still exposed with a mild increase in the surface area coverage. Asterisks: newly formed bone. (D) showing a higher magnification of the newly formed woven bone with randomly oriented collagen bundles with many osteoblast prints (red arrows). Opening of a newly formed neurovascular canal was also seen (yellow arrow). R: exposed root surface. (original magnification A & Cx 50, Bx 200, Dx750).

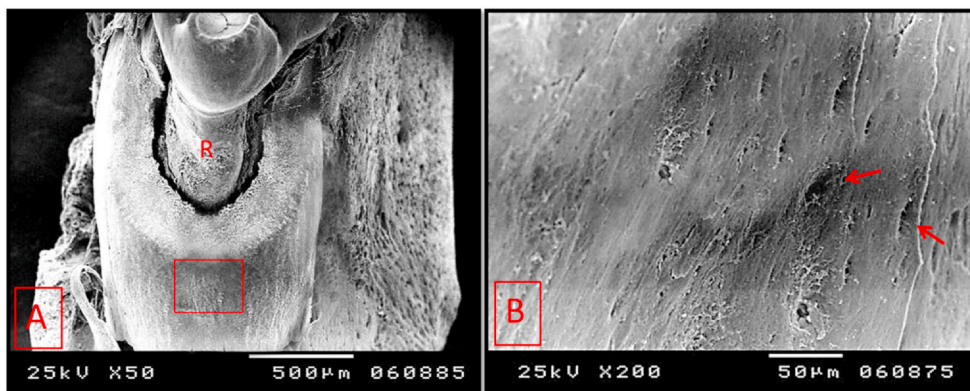


**Fig. 10.** Scanning electron micrographs of group II (2 weeks period). (A); The newly formed bone almost covered the apical half of the root surface. (B); A higher magnification of the boxed area of A showing somewhat smooth outer surface of the newly formed bone containing orifices of neurovascular canals with irregular outline (arrows). R: exposed root surface. (original magnification A×50, Bx200).

In 4 weeks period, SEM analysis showed complete coverage of the mesial root surface by a thin bony layer (Fig. 11-A). On a higher magnification, the new bone showed dense lamellar structure with much improvement of the overall surface texture and smoothness. Also, few Howship's lacunae could be seen (Fig. 11-B). The newly formed bone in cervical region appeared to have a rough texture with many newly formed neurovascular canals and small openings representing entrance to osteocyte lacunae (Fig. 11-C). Almost complete re-establishment of the normal relationship was detected between the alveolar bone proper of the newly formed mesial wall of the alveolar socket and its supporting alveolar bone (Fig. 11-D).

In group III, after 2 weeks, a relatively thick layer of newly formed bone was seen covering the mesial root surface extending from the root apex until cervical region. While some areas of the regenerated bone showed mature dense lamellar structure with smooth surface and well defined neurovascular canals, other areas had rough surface and contained what is called osteoid packets with reduced electron backscattering properties (Fig. 12).

In 4 weeks period, almost complete healing of the periodontal defect was observed. The bony wall restored almost its full thickness running

homogenously with outer and inner cortical plates. A closer view showed the majority of regenerated bone with smooth mature lamellar surface containing regularly outlined and well defined openings of the neurovascular canals. However, few areas had rough surface with many Howship's lacunae (Fig. 13).

### 3.3. Statistical analyses

#### 3.3.1. Histomorphometric analysis of new bone surface area

Using ANOVA test, A highly significant difference (\*\*) was found between groups in both 2 and 4 weeks follow up periods (Table 1). By post hoc test, a significant difference (\*) was found between group I and group II and between group I and group III in 2 weeks follow up period. In 4 weeks follow up period, the difference between group I and group II was significant (\*) while it was highly significant (\*\*) between group I and group III. The difference between group II and group III was non significant (NS) in 2 weeks and significant (\*) in 4 weeks follow up periods (Table 2).

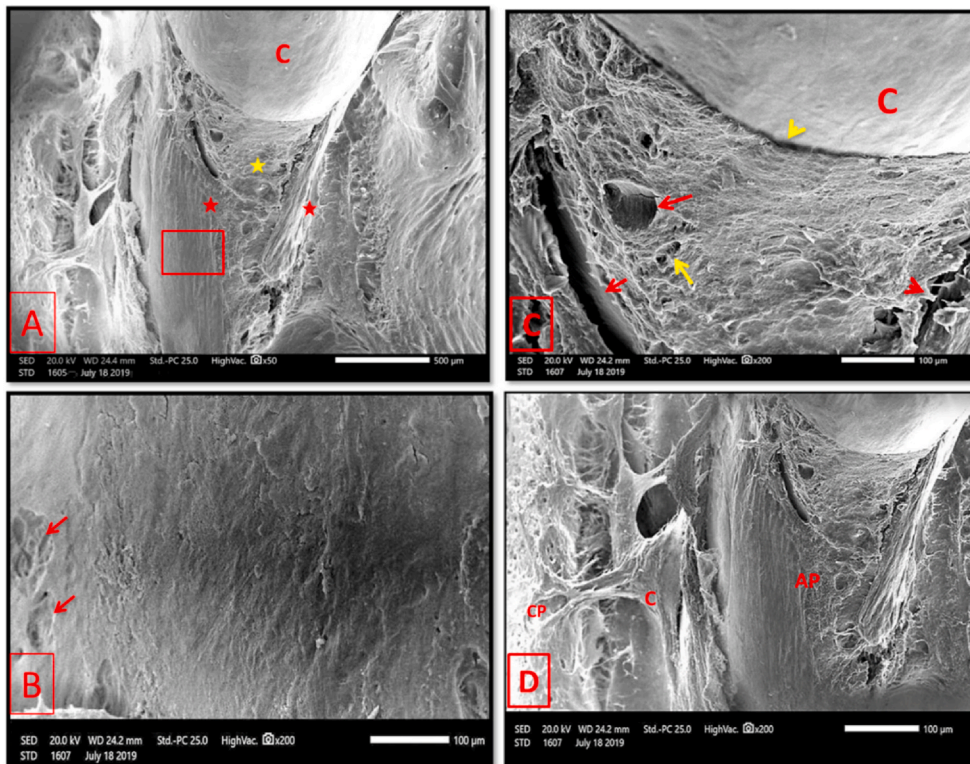


**Fig. 11.** Scanning electron micrographs of group II (4 weeks period). (A) The mesial root surface was covered by thin bony layer (yellow asterisk) that was increasing in thickness by crawling of the next growing layer buccally and lingually (red asterisks). C: 1st molar crown. (B) A higher magnification of the boxed area of A showing dense lamellar bone with few Howship's lacunae (arrows). (C) A higher magnification of the cervical region showing complete root coverage with new bone of rough texture. Newly formed neurovascular canals (red arrows) and small openings representing entrance to osteocyte lacunae were seen (yellow arrow). A complete coverage of the root surface until tooth cervix was evident (yellow arrowhead). red arrowhead: Crack in new bone. (D) showing almost complete regeneration of normal relationship between newly formed mesial wall of alveolar bone proper and supporting alveolar bone. AP: alveolar bone proper, C: cancellous part of supporting alveolar bone, CP: cortical plate of supporting alveolar bone. (original magnification A×50, B, C & Dx200).

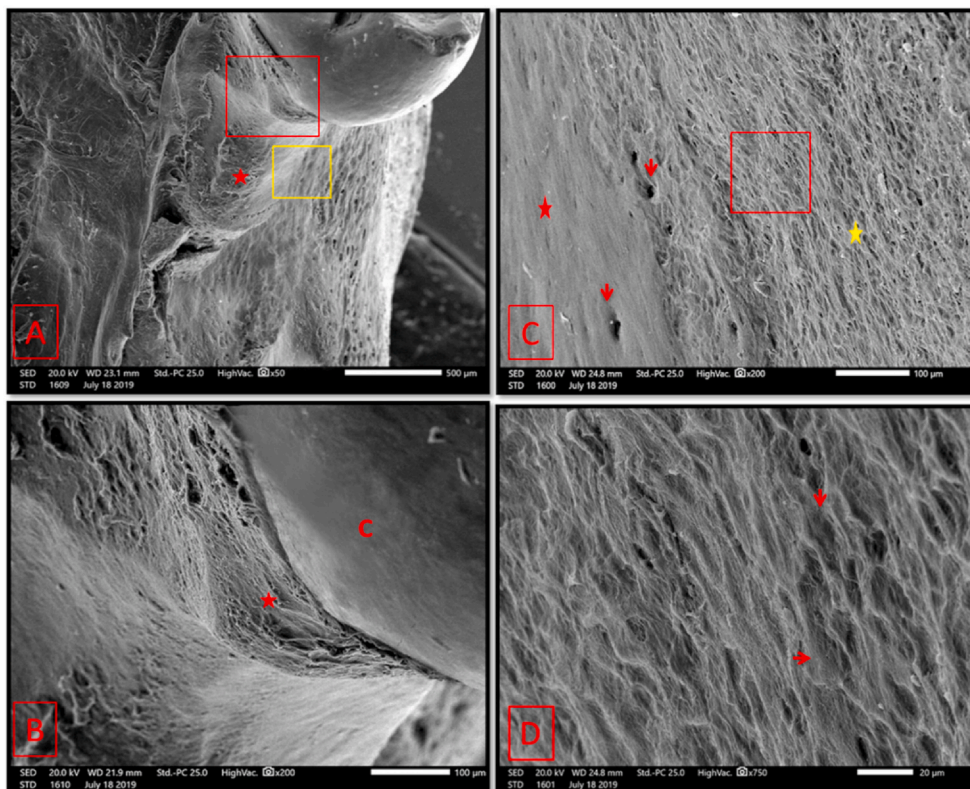


**Fig. 12.** Scanning electron micrographs of group III (2 weeks period). (A); A relatively thick layer of newly formed bone covered the mesial root surface (asterisk). (B); A higher magnification of the red boxed area of A showing complete coverage of the root surface until the tooth cervix (asterisk). C: 1st molar crown. (C); A higher magnification of the yellow boxed area of A showing areas of smooth surfaced (red asterisk) & rough surfaced (yellow asterisk) bone with detection of neurovascular canals' openings in both (arrows). (D); A higher magnification of the boxed area of A showing osteoid packets, with reduced electron back-scattering properties, and shallow depression made by osteoblasts on its surface (red arrows). (original magnification A×50, B & Cx 200, Dx750).

### 3.3.2. Anti-PCNA immunohistochemical statistical analysis

A non significant statistical difference (<sup>NS</sup>) was found between the numbers of anti-PCNA positive nuclei of the three groups in both time intervals. However, the anti-PCNA counting was highest in group III followed by group II and lowest in group I (Table 3).

## 4. Discussion

In our study, we emphasized the potential role of ozone gel compared with PRF membrane in periodontal regeneration using an intrabony periodontal defect in rats. For this purpose, acute model of



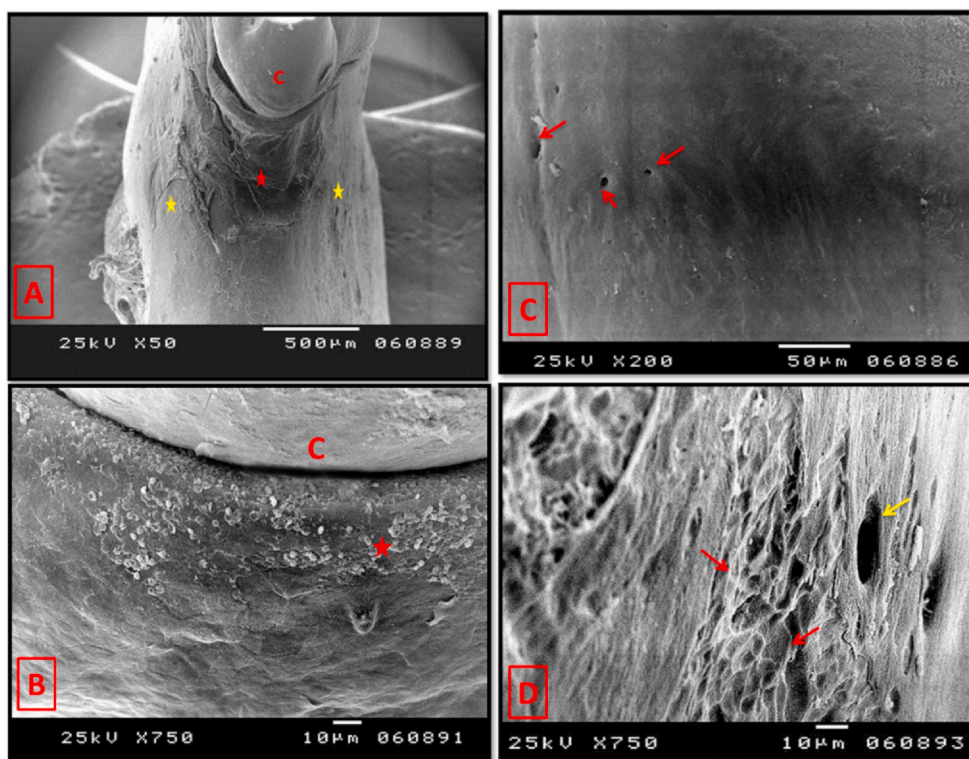


**Fig. 13.** Scanning electron micrograph of group III (4 weeks period) (A); showing almost complete healing of the mesial wall of alveolar bone (red asterisk) running homogeneously with outer and inner cortical plates (yellow asterisks). (B) showing complete formation and normal positioning of the alveolar crest (asterisk). C: 1st molar crown. (C) showing smooth surface of the regenerated mature lamellar bone. Note the regularly outlined openings of the neurovascular canals (arrows). (D) Some areas of lamellar bone were rough surfaced with many Howship's lacunae (red arrows). Yellow arrow: neurovascular canal opening. (original magnification A×50, B & Dx750, Cx200).

**Table 1**

Comparison between Mean ± S.D values of the surface area of newly formed alveolar bone in group I, group II and group III using ANOVA test.

Surface area of new bone				
Parameters	Mean ± S.D	Min –Max	F	p-value
Group I (2 ws)	305.94 ± 37.66	250.62–359.18	17.751	0.000**
Group II (2 ws)	357.04 ± 21.15	330.56–395.16		
Group III (2 ws)	394.51 ± 46.29	333.58–452.16		
Group I (4 ws)	309.06 ± 36.19	250.62–359.02	22.492	0.000**
Group II (4 ws)	383.26 ± 42.34	333.58 ± 454.82		
Group III (4 ws)	470.26 ± 85.54	333.58–553.05		

**Table 2**

Comparison between Mean ± S.D values of the surface area of newly formed alveolar bone in group I, group II and group III using post hoc test.

Surface area of new bone		
Parameters	Group I (2 ws)	Group II (2 ws)
Group I (2 ws)	_____	_____
Group II (2 ws)	0.005*	_____
Group III (2 ws)	0.001*	0.051 <sup>NS</sup>
Parameters	Group I (4 ws)	Group II (4 ws)
Group I (4 ws)	_____	_____
Group II (4 ws)	0.011*	_____
Group III (4 ws)	0.000**	0.003*

surgically created periodontal defect was chosen and this is because although the chronic model, using ligature, indeed create a diseased root surface, it still not identical to the naturally occurring periodontitis in addition to the fact that the obtained defect size and shape are uncontrollable.<sup>51</sup> Unlikely, these parameters are more controlled in the surgically created acute model thus help to create a reproducible defect model to test and compare between treating materials without any significant bias.<sup>52</sup>

The three wall periodontal defect model, that was previously

**Table 3**

Comparison between Mean ± S.D values of the number of anti-PCNA positive nuclei in group I, group II and group III using ANOVA test.

Anti-PCNA statistical results				
Parameters	Mean ± S.D	Min –Max	F	p-value
Group I (2 ws)	74.83 ± 8.53	55–85	1.820	0.178 <sup>NS</sup>
Group II (2 ws)	80.83 ± 13.29	60–99		
Group III (2 ws)	83 ± 10.23	69–96		
Group I (4 ws)	72.58 ± 5.98	65–85	1.748	0.190 <sup>NS</sup>
Group II (4 ws)	78.33 ± 15.85	56–99		
Group III (4 ws)	81.33 ± 10.97	65–95		

adopted in many studies,<sup>48,53,54</sup> was applied here. This is because the fact that although this type of intrabony defects is considered the ideal one for regenerative procedures,<sup>55</sup> it had proved to be a defect with a limited spontaneous healing.<sup>54</sup>

In group I, in both follow up periods, almost all signs of periodontal injury were demonstrated including inflammatory cell infiltration, root and alveolar bone resorption and enlargement of the defect area as reported in previous studies.<sup>55,56</sup> This was attributed to the pathogenesis of periodontal inflammatory process which involves the release of inflammatory mediators, including prostaglandins and cytokines, IL-1 and TNF-α, causing recruitment of inflammatory cells, elaboration of lytic enzymes and osteoclastic differentiation leading ultimately to connective tissue destruction, progressive alveolar bone resorption with subsequent enlargement of the periodontal defect.<sup>58,59</sup> The detected mild new woven bone formation was also previously seen by Takeuchi T et al.<sup>60</sup> In 4 weeks period, the observed mild new woven bone formation with non-functionally oriented collagen fibers came in agreement with observations seen in earlier studies.<sup>52,60</sup> Interestingly, the newly formed bony island that was found to almost reach the root surface was indicative of future ankylosis. This was also recorded by Melcher AH et al.<sup>61</sup> who found a bony callus invading the defective PDL area with development of ankylosis between bone and tooth within 2:4 weeks after defect induction.

In **group II**, the observed new alveolar bone formation with apparent osteoblastic activity came in agreement with the finding of both Akpınar et al.<sup>62</sup> and Ozdemir et al.<sup>63</sup> In Akpınar et al. study, he accredited the new bone formation to the ability of ozone to increase the osteoblastic activity that was found to be significantly higher in ozone treated group than the untreated group. Another added reason is that ozone enhances bone morphogenic protein-2 (BMP-2) expression<sup>64</sup> and alkaline phosphatase (ALP) enzyme activity<sup>65</sup> in osteoblasts thus having a positive effect on bone formation and mineralization respectively. Furthermore, the reported new functionally oriented PDL collagen fibers formation together with the obvious fibroblastic activity was similar to the findings of Kazancıoğlu et al.<sup>66</sup> who found that topical ozone application, in addition to enhancing bone formation, it promoted fibrous connective tissue formation with abundant new collagen fibers and numerous fibroblasts. This was attributed to the angiogenetic along with biosynthetic abilities of ozone through which it can activate cellular proliferation and protein synthesis thus elevate the functional activity of cells and regeneration potential of tissues and organs.<sup>67</sup> Also, Wang PL et al. study<sup>68</sup> had evaluated the effect of ozone ointment on type-I collagen production ability of human gingival fibroblasts which is directly linked to the regenerative capacity of periodontal tissues. It showed that ozone indeed boosted the production of type-I collagen by approximately 1.4-fold and, consequently, thought to have a positive effect on the reconstruction of periodontal tissues.

In **group III**, the regenerated bone with mature dense lamellar structure outlined with active plump osteoblasts came in accordance with the results of Du J et al. study.<sup>69</sup> Our explanation depends on Eduardo A et al. study<sup>70</sup> that evaluated the effect of platelet derived growth factors on the alveolar bone osteoblasts' bone forming potential. It was observed that these osteoblasts showed an increased rate of cellular proliferation by 3.8-fold with a significant increase in cellular migration and chemotaxis by 9.6 fold than the control group. Remarkably, this increased cellular proliferation and migration was accompanied with an overall increase in the cellular synthesis of extracellular matrix components with increased osteoblastic expression of procollagen type I and ALP suggesting an accelerated rate of matrix formation and mineralization respectively. Additionally, Li Q. et al.<sup>71</sup> had found that PRF almost equaled the osteogenic medium in its effect on mineralization behavior of cultured periodontal progenitor cells with a highly significant increase in ALP activity and a 4.9 fold increase in the degree of matrix mineralization.

The restoration of normal architecture of PDL with regeneration of different groups of dense collagen bundles of PDL was similar to Du J et al.<sup>69</sup> study. This result was accredited to the ability of PRF membrane to slowly release a set of growth factors, including PDGF, TGF- $\beta$ 1, IGF, FGF& VEGF,<sup>35</sup> that could enhance cell proliferation and extracellular matrix synthesis thus promote wound healing and regeneration of periodontal tissues.<sup>72</sup> Furthermore, PRF membrane proved to have excellent biodegradability with enhancement of collagen formation.<sup>71</sup>

In addition, the regenerated DGJ, recorded in this group, was attributed to the sustained release of epidermal growth factor from the activated platelets of the PRF membrane that enhances epithelialization.<sup>73</sup>

The histomorphometric analysis of the total new bone surface area showed a significant difference of the area of new bone formation between group I and group II in both 2 and 4 weeks follow up periods. The difference between group I and group III was significant in 2 weeks period and highly significant in 4 weeks period. The differences detected between the 2 and 4 weeks periods of each group were non-significant in group I and significant in both group II and III.

The immunohistochemical statistical analysis showed an increase in the total number of anti PCNA positive nuclei in both group II and III than group I with the PRF group being the highest, however, the difference between groups was not significant at both time intervals. These findings were justified by two reasons. Primarily, the proliferative cellular process was present in all groups but the anti PCNA

positive nuclei of group I was mainly related to the intense inflammatory infiltration occupying the periodontal defect and was not close enough to the bone surface to express actual healing. Secondly, both ozone and PRF had proved, as previously mentioned, to significantly enhance cellular differentiation so, most of the cells of both groups were already in the differentiation phase with negative anti PCNA expression while the cells of the untreated specimens of group I still in the cell proliferation phase.

In conclusion, our presented histological and immunohistochemical results could be considered as an additional clue that amplify the regenerative capacity of both ozone and PRF on periodontal healing with the PRF being better however, further multi-institutional histological and clinical studies with different parameters are required to confirm this possibility.

## Declaration of competing interest

None.

## References

1. Skoog DA, Holler FJ, Crouch SR. sixth ed. *Principles of Instrumental Analysis*. vol. 9. Thomson Brooks/Cole; 2007.
2. Manbachi A, Cobbold RSC. Development and application of piezoelectric materials for ultrasound generation and detection. *Ultrasound*. 2011;19(4):187–196.
3. Kumar GS. *Orban's Oral Histology and Embryology*. thirteenth ed. Elsevier; 2011:172.
4. Burt B. Science and therapy committee of the American academy of periodontology. Position paper: epidemiology of periodontal diseases. *J Periodontol*. 2005;76(8):1406–1419.
5. Pihlstrom BL, Michalowicz BS, Johnson NW. Periodontal diseases. *Lancet*. 2005;366(9499):1809–1820.
6. Kinane DF, Stathopoulou PG, Papapanou PN. Periodontal diseases. *Nat Rev Dis Primers*. 2017;3(1):17038.
7. Froum S. J. Periodontal healing following open debridement flap procedure I: clinical assessment of soft tissue and osseous repair. *J Periodontol*. 1981;53(1):8–14.
8. Elumalai M, Natarajan PM. Wound healing in periodontics. *Biosci Biotechnol Res Asia*. 2014;11(2):791–796.
9. Kaner D, Soudan M, Zhao H, Gabmann G, Schonhauser A, Friedmann A. Early healing events after periodontal surgery: observations on soft tissue healing, microcirculation, and wound fluid cytokine levels. *Int J Mol Sci*. 2017;18(2):283.
10. Chen FM, Jin Y. Periodontal tissue engineering and regeneration: current approaches and expanding opportunities. *Tissue Eng B Rev*. 2010;16(2):219–255.
11. Reynolds MA, Aichelmann-Reidy ME, Branch-Mays GL. Regeneration of periodontal tissue: bone replacement grafts. *Dent Clin*. 2010;54(1):55–71.
12. Villar CC, Cochran DL. Regeneration of periodontal tissues: guided tissue regeneration. *Dent Clin*. 2010;54(1):73–92.
13. Cortellini P, Labriola A, Tonetti MS. Regenerative periodontal therapy in intrabony defects: state of the art. *Minerva Stomatol*. 2007;56(10):519–539.
14. Bosshardt DD, Sculean A. Does periodontal tissue regeneration really work? *Periodontol*. 2000;51(1):208–219 2009.
15. Trombelli L. Which reconstructive procedures are effective for treating the periodontal intraosseous defect? *Periodontol*. 2000;37(1):88–105 2005.
16. Sansriti T, Suyog J. Dental applications of ozone therapy: a review of literature. *Saudi J Dent Res*. 2017;8(1-2):105–111.
17. Sen CK, Roy S. Redox signals in wound healing. *Biochim Biophys Acta*. 2008;1780(11):1348–1361.
18. Seidler VI. Ozone and its usage in general medicine and dentistry. *Prague Med Rep*. 2008;109(1):5–13.
19. Broadwater WT, Hoehn RC. Sensitivity of three selected bacterial species to ozone. *Appl Microbiol*. 1973;26(3):391–393.
20. Chang Hubert, Lynch Edward, Grootveld Martin. Oxidative consumption of oral biomolecules by therapeutically-relevant doses of ozone. *Adv Chem Eng Sci*. 2012;2(2):238–245.
21. Srinivasan SR, Amaechi BT. Ozone: a paradigm shift in dental therapy. *J Global Oral Health*. 2019;2(1):68–77.
22. Jakab GJ, Spannhake EW, Canning BJ, Kleeburger SR, Gilmour MI. The effects of ozone on immune function. *Environ Health Perspect*. 1995;103(2):77–89.
23. Srinivasan K. The application of ozone in dentistry: a systematic review of literature. *Sch J Dent Sci*. 2015;2(6):373–377.
24. Gopalakrishnan S, Parthiban S. Ozone: a new revolution in dentistry. *J Bio Innovat*. 2012;1(3):58–69.
25. Kumar A, Bhagawati S, Tyagi P, Kumar P. Current interpretations and scientific rationale of ozone usage in dentistry: a systematic review of literature. *Eur J Gen Dent*. 2014;3(3):175–180.
26. Ebensberger U, Pohl Y, Filippi A. PCNA-expression of cementoblasts and fibroblasts on the root surface after extra oral rinsing for decontamination. *Dent Traumatol*. 2002;18(5):262–266.
27. Pattanaik B, Jetwa D, Pattanaik S, Manglekar S, Naitam DN, Dani A. Ozone therapy in dentistry: a literature review. *J Interdiscip Dent*. 2011;1(2):87–92.

28. Chandran P, Sivasdas A. Platelet-rich fibrin: its role in periodontal regeneration. *Saudi J for Dent Res.* 2014;5(2):117–122.
29. Miron RJ. *Choukroun J. Platelet Rich Fibrin in Regenerative Dentistry: Biological Background and Clinical Indications.* first ed. John Wiley & Sons Ltd; 2017.
30. Dangaria SJ, Ito Y, Walker C, Druzinsky R, Luan X, Diekwisch TJ. Extracellular matrix-mediated differentiation of periodontal progenitor cells. *Differentiation.* 2009;78(2-3):79–90.
31. Dangaria SJ, Ito Y, Luan X, Diekwisch TJ. Successful periodontal ligament regeneration by periodontal progenitor preceeding on natural tooth root surfaces. *Stem Cell.* 2011;20(10):1659–1668.
32. Hollander A, Macchiarini P, Gordijn B, Birchall M. The first stem cell-based tissue-engineered organ replacement: implications for regenerative medicine and society. *Regen Med.* 2009;4(2):147–148.
33. Choukroun J, Adda F, Schoeffer C, Vervelle A. PRF: an opportunity in perio-implantology. *Implantodontie.* 2001;42:55–62.
34. Dohan DM, Choukroun J, Diss A. Platelet-rich fibrin (PRF): a second-generation platelet concentrate. Part II: platelet related biologic features. *Oral Surg Oral Med Oral Pathol Oral Radiol Endod.* 2006;101(3):45–50.
35. Dohan DM, Choukroun J, Diss A, et al. Platelet-rich fibrin (PRF): a second-generation platelet concentrate. Part III: leucocyte activation: a new feature for platelet concentrates? *Oral Surg Oral Med Oral Pathol Oral Radiol Endod.* 2006;101(3):51–55.
36. Sharma A, Pradeep AR. Treatment of 3-wall intrabony defects in patients with chronic periodontitis with autologous platelet rich fibrin: a randomized controlled clinical trial. *J Periodontol.* 2011;82(12):1705–1712.
37. Thorat M, Pradeep AR, Pallavi B. Clinical effect of autologous platelet-rich fibrin in the treatment of intra-bony defects: a controlled clinical trial. *J Clin Periodontol.* 2011;38(10):925–932.
38. Diss A, Dohan DM, Mouhyi J, Mahler P. Osteotome sinus floor elevation using Choukroun's platelet-rich fibrin as grafting material: a 1-year prospective pilot study with micro threaded implants. *Oral Surg Oral Med Oral Pathol Oral Radiol Endod.* 2008;105(5):572–579.
39. Horowitz RA, Del Corso M, Prasad HS, Rohrer M D, Dohan Ehrenfest DM. Sinus floor augmentation with simultaneous implant placement using Choukroun's platelet rich fibrin as the sole grafting material: a radiologic and histologic study at 6 months. *J Periodontol.* 2009;80(12):2056–2064.
40. Dohan Ehrenfest DM, Peppo GM, Doglioli P, Sammartino G. Slow release of growth factors and thrombospondin-1 in Choukroun's platelet-rich fibrin (PRF): a gold standard to achieve for all surgical platelet concentrates technologies. *Growth Factors.* 2009;27(1):63–69.
41. Li Q, Geng Y, Lu L, Yang T, Zhang M, Zhou Y. Platelet-rich fibrin-induced bone marrow mesenchymal stem cell differentiation into osteoblast-like cells and neural cells. *Neural Regen Res.* 2011;6(31):2419–2423.
42. Chang IC, Tsai CH, Chang YC. Platelet-rich fibrin modulates the expression of extracellular signal-regulated protein kinase and osteoprotegerin in human osteoblasts. *J Biomed Mater Res.* 2010;95(1):327–332.
43. Huang FM, Yang SF, Zhao JH, Chang YC. Platelet-rich fibrin increases proliferation and differentiation of human dental pulp cells. *J Endod.* 2010;36(10):1628–1632.
44. Raja S, Byakod G, Pudakalkatti P. Growth factors in periodontal regeneration. *Int J Dent Hyg.* 2009;7(2):82–89.
45. Giannobile WV, Hernandez RA, Finkelman RD. Comparative effects of platelet-derived growth factor-BB and insulin-like growth factor-I, individually and in combination on periodontal regeneration in Macaca fascicularis. *J Periodontol Res.* 1996;31(5):301–312.
46. Annunziata M, Oliva A, Buonaiuto C, Di Feo A, Di Pasquale R, Passaro I. In vitro cell-type specific biological response of human periodontally related cells to platelet-rich plasma. *J Periodontol Res.* 2005;40(6):489–495.
47. Xuejing D, Zhiyong L, Xiujuan L. Study of platelet-rich fibrin combined with rat periodontal ligament stem cells in periodontal tissue regeneration. *J Cell Mol Med.* 2018;22(2):1047–1055.
48. Yu N, Oortgiesen DA, Bronckers AL, Yang F, Walboomers XF, Jansen JA. Enhanced periodontal tissue regeneration by periodontal cell implantation. *J Clin Periodontol.* 2013;40(7):698–706.
49. Zang Sheng-Qi, Kang Shuai, Hu Xin, Wang Meng. Comparison of different periodontal healing of critical size noncontained and contained intrabony defects in beagles. *Chin Med J.* 2017;130(4):477–486.
50. Theodoro LH, Ferro-Alves ML, Longo M. Curcumin photodynamic effect in the treatment of the induced periodontitis in rats. *Laser Med Sci.* 2017;32(8):1783–1791.
51. Eslami B, Behnia H, Javadi H, Khiabani KS, Saffar AS. Histopathologic comparison of normal and hyperplastic condyles. *Oral Surg Oral Med Oral Pathol Oral Radiol Endod.* 2003;96(6):711–717.
52. Yan XZ, Jeroen JJP, van den Beucken JJ, et al. Periodontal tissue regeneration using enzymatically solidified chitosan hydrogels with or without cell loading. *Tissue Eng.* 2015;21(5-6):1066–1076.
53. Oortgiesen DA, Walboomers XF, Bronckers AL, Meijer GJ, Jansen JA. Periodontal regeneration using an injectable bone cement combined with BMP-2 or FGF-2. *J Tissue Eng Regen Med.* 2014;8(3):202–209.
54. Oortgiesen DA, Meijer GJ, Bronckers AL, Walboomers XF, Jansen JA. Regeneration of the periodontium using enamel matrix derivative in combination with an injectable bone cement. *Clin Oral Invest.* 2013;17(2):411–421.
55. Pellegrini G, Seol YJ, Gruber R, Giannobile WV. Pre-clinical models for oral and periodontal reconstructive therapies. *J Dent Res.* 2009;88(12):1065–1076.
56. Lekic P, Klausen B, Friis-Hasche E, Beloica D, Knezevic M, Hougen HP. Influence of age and immunization on development of gingivitis in rats. *Acta Odontol Scand.* 1989;47(4):233–238.
58. De Lima V, Bezerra MM, de Menezes Alencar VB. Effects of chlorpromazine on alveolar bone loss in experimental periodontal disease in rats. *Eur J Oral Sci.* 2000;108(2):123–129.
59. Bezerra MM, de Lima V, Alencar VB. Selective cyclooxygenase-2 inhibition prevents alveolar bone loss in experimental periodontitis in rats. *J Periodontol.* 2000;71(6):1009–1014.
60. Takeuchi T, Bizenjima T, Ishii Y, Imamura K. Enhanced healing of surgical periodontal defects in rats following application of a self-assembling peptide nanofibre hydrogel. *J Clin Periodontol.* 2016;43(3):279–288.
61. Melcher AH. Repair of wounds in the periodontium of the rat. Influence of periodontal ligament on osteogenesis. *Arch Oral Biol.* 1970;15(12):1183–1198.
62. Akpınar A, Çalıřır M, Poyraz O, Göze F. The effects of ozone on the local and systemic interleukin 1 $\beta$  (IL-1 $\beta$ ) and IL-10 levels experimental periodontitis model in rats. *Cumhuriyet Med J.* 2017;39(3):608–619.
63. Ozdemir H, Toker H, Balci H, Ozer H. Effect of ozone therapy on autogenous bone graft healing in calvarial defects: a histologic and histometric study in rats. *J Periodontol Res.* 2013;48(6):722–726.
64. Alpan AL, Toker H, Ozer H. Ozone therapy enhances osseous healing in rats with diabetes with calvarial defects: a morphometric and immunohistochemical study. *J Periodontol.* 2016;87(8):982–989.
65. Renno AC, McDonnell PA, Parizotto NA, Laakso EL. The effects of laser irradiation on osteoblast and osteosarcoma cell proliferation and differentiation in vitro. *Photomed Laser Surg.* 2007;25(4):275–280.
66. Kazancioglu HO, Ezirganli S, Aydin MS. Effects of laser and ozone therapies on bone healing in the calvarial defects. *J Craniofac Surg.* 2013;24(6):2141–2146.
67. Kim HS, Noh SU, Han YW, et al. Therapeutic effects of topical application of ozone on acute cutaneous wound healing. *J Korean Med Sci.* 2009;24(3):368–374.
68. Wang PL, Tachi Y, Masuno K, Okusa N, Imamura Y. The study of ozone ointment on human gingival fibroblasts cell proliferation ability and anti-inflammatory. *J Hard Tissue Biol.* 2018;27(3):209–212.
69. Du J, Mei S, Guo L, Su Y, Wang H, Liu Y. Platelet-rich fibrin/ aspirin complex promotes alveolar bone regeneration in periodontal defect in rats. *J Periodontol Res.* 2018;53(1):47–56.
70. Anitua E, Tejero R, Zalduendo MM, Orive G. Plasma rich in growth factors promotes bone tissue regeneration by stimulating proliferation, migration, and autocrine secretion in primary human osteoblasts. *J Periodontol.* 2013;84(8):1180–1190.
71. Li Q, Pan S, Dangaria SJ, et al. Platelet-rich fibrin promotes periodontal regeneration and enhances alveolar bone augmentation. *BioMed Res Int.* 2013;2013(10):638043 13pages.
72. Mullaguri H, Suresh N, Surendran S, Velmurugan N, Chitra S. Role of pH changes on transforming growth factor- $\beta$ 1 release and on the fibrin architecture of platelet-rich fibrin when layered with bio-dentine, glass ionomer cement, and intermediate restorative material. *J Endod.* 2016;42(5):766–770.
73. Boyapati L, Wang HL. The role of platelet-rich plasma in sinus augmentation: a critical review. *Implant Dent.* 2006;15(2):160–170.